

1 Road impacts from the 2016 Kaikōura earthquake: an analogue for a future Alpine Fault 2 earthquake?

3
4 Tom R Robinson

5 Department of Geography, Durham University, Durham, UK

6 Tom.robinson@durham.ac.uk

7 8 **Abstract**

9 The 2016 M_w 7.8 Kaikōura earthquake involved complex rupture of multiple faults for > 170 km,
10 generating strong ground shaking throughout the upper South Island leading to widespread
11 landsliding. As a result of surface fault rupture and landslides, State Highway 1 and State Highway
12 70 were blocked, isolating Kaikōura and the surrounding communities and necessitating
13 evacuations by air and sea. In all these respects the Kaikōura earthquake can be considered an
14 analogue for a future Alpine Fault earthquake, providing lessons for the necessary emergency
15 response. Landslide blockages primarily occurred where surrounding slopes averaged > 18° and
16 where Peak Ground Acceleration was > 0.43 g, Peak Ground Velocity > 41 cm/s, or Modified
17 Mercalli Intensity > 7.9. Using a potential future Alpine Fault scenario earthquake, this study
18 identifies locations on other key state highway routes that have similar predictive variables that
19 may therefore become blocked in a future earthquake. This suggests that SH6 between Hokitika
20 and Haast, State Highway 73 near Arthur's Pass, and State Highway 94 south of Milford Sound
21 are all likely to be affected. This will necessitate the evacuation of large numbers of spatially
22 distributed tourists as well as the resupply of isolated local populations. The possibility of bad
23 weather along with a lack of sea ports south of Hokitika will likely make such activities challenging.
24 Contingency planning based on experiences from the Kaikōura earthquake is therefore necessary
25 and likely to prove invaluable following an Alpine Fault earthquake.

26

27 **Keywords:** Earthquakes, Landslides, Hazard modelling, Risk analysis, Emergency response.

28

29 **1 INTRODUCTION**

30 The 14 November 2016 M_w 7.8 Kaikōura earthquake was the largest to strike New Zealand
31 since 2009. The earthquake involved complex rupture of over 20 previously known and unknown
32 faults in the upper South Island (Hamling et al., 2017) and propagated > 170 km north from the
33 epicentre near Waiiau (Fig. 1). With rupture initiating at a depth of just 15 km, the earthquake
34 resulted in strong ground shaking (> 1g) throughout the upper South Island and lower North Island
35 (Kaiser et al., 2017). The affected region is steep and mountainous, rising from sea-level to over
36 2,500 m in ~20 km. Consequently, > 10,000 landslides are thought to have occurred resulting in >
37 190 landslide dams (Massey et al., 2018). Despite its mountainous nature, the region is an
38 important transport corridor linking Christchurch, Kaikōura, Blenheim, and Picton via State

39 Highway (SH) 1. Consequently, the earthquake caused substantial impacts in the form of
40 landslides and surface fault rupture blocking SH1, causing Kaikōura to be cut-off from the rest of
41 the South Island. These road blockages resulted in the road being closed for ~1 year (Mason et al.
42 2017), although closures due to heavy rainfall and further landsliding continue to occur at the time
43 of writing. A full description of the damage caused by the event has been summarised by
44 numerous authors in an NZSEE Special Issue (e.g. Orense et al., 2017; Cubrinovski et al., 2017;
45 Palermo et al., 2017; Liu et al., 2017).

46 The impacts from the Kaikōura earthquake are in many respects a potential analogue for
47 the impacts resulting from a future rupture of the Alpine Fault (Fig. 1). This oblique strike-slip fault
48 runs along the western edge of the Southern Alps for c. 411 km ($\pm 10\%$) and forms the onshore
49 plate boundary between the Australian and Pacific plates, sustaining a slip rate of 27 ± 5 mm/yr.
50 The Alpine Fault has generated large ($M_w 8.1 \pm 0.2$) earthquakes regularly over the last 8,000
51 years, with a relatively invariable average recurrence of ~341 years or less (Berryman et al., 2012;
52 Stirling et al., 2012; Howarth et al., 2016; Cochran et al., 2017). The last known Alpine Fault
53 earthquake occurred in 1717 AD (Yetton, 1998; Wells et al., 1999; Howarth et al., 2012; De
54 Pascale & Langridge, 2012) giving an ~26% conditional probability of rupture in the next 50 years
55 (Biasi et al., 2015). Such an earthquake is expected to be $M_w \sim 8.0$, have a rupture length > 200
56 km, initiate at shallow (<15 km) depth and, consequently, generate strong ground shaking
57 throughout the affected area (Fig. 1) resulting in widespread landsliding (Robinson & Davies, 2013;
58 Robinson et al., 2016). Like the Kaikōura area, the West Coast Region, where the Alpine Fault is
59 located, forms a narrow coastal strip between the Tasman Sea and the Southern Alps. The region
60 is rural, sparsely populated, and relatively inaccessible: only one road (SH6) traverses the region,
61 and only three roads (SH6, SH7, & SH73) cross the Southern Alps connecting it with the rest of the
62 South Island (Fig. 1). These routes navigate through steep and narrow Alpine Passes (Arthur's
63 Pass, Lewis Pass and Haast Pass) and cross the Alpine Fault at multiple locations. Consequently,
64 there is a potential for substantial disruption to these routes from landslides and other ground
65 damage triggered by an Alpine Fault earthquake. Thus, despite significant differences in the
66 seismological factors between the Kaikōura earthquake and a future Alpine Fault earthquake, the
67 former presents an opportunity to learn from its impacts and the subsequent emergency response
68 and formulate effective response and recovery plans for a future Alpine Fault earthquake.

69 Using observations of road impacts from the 2016 Kaikōura earthquake, this study aims to
70 envisage the potential road impacts resulting from a future rupture of the Alpine Fault. The
71 conditions under which road blockages resulted in the Kaikōura event are investigated and
72 subsequently an analysis of where similar conditions exist along road networks is undertaken.
73 Using a scenario Alpine Fault earthquake, the locations where roads are liable to blockages are
74 identified along with any resulting isolated areas. Reflecting on the experience of the Kaikōura
75 earthquake, a discussion of the potential emergency response requirements is provided.

76

77 **2 METHODS & DATA**

78 The primary form of road impacts in the Kaikōura earthquake resulted from fault rupture and
79 landslides (Mason et al., 2017; Davies et al., 2017; Stirling et al., 2017; Dellow et al., 2017). By
80 assessing the locations where road impacts occurred in this event, it may be possible to identify
81 sections of road elsewhere in the South Island with similar conditions that may therefore suffer
82 impacts in a future earthquake on other faults (e.g. the Alpine Fault). This study uses road
83 blockage data collected by NZTA in the immediate aftermath of the Kaikōura earthquake and is
84 therefore assumed to have resulted from the mainshock only. The data captures full and partial
85 blockages of major public roads but does not include data on private roads or 4x4 tracks. The
86 study area encompasses the region outlined in Fig. 1, which captures the region of South Island
87 exposed to shaking greater than MMI 6.

88

89 **2.1 Fault rupture impacts**

90 Due to the number and complexity of surface fault ruptures in the Kaikōura earthquake (Stirling et
91 al., 2017), multiple sections of both SH1 and SH70 were directly affected by surface fault rupture
92 (Fig. 1). Where surface ruptures intersected these roads, the road surface was displaced, with
93 vertical displacements in particular making the road impassable (see Stirling et al., 2017 and
94 Davies et al., 2017 for examples). Identifying potential sites of future fault rupture impacts for an
95 Alpine Fault earthquake requires identifying locations where other roads intersect the proposed
96 surface rupture trace. Given uncertainties in accurately locating a fault surface trace, this study
97 considers any road within 50 m of the known surface trace of the Alpine Fault to be potentially
98 affected by surface fault rupture. It should be highlighted however, that such an approach is only
99 applicable for known faults and surface traces. During the Kaikōura earthquake, surface fault
100 rupture occurred on several previously unknown faults and fault traces (Stirling et al., 2017). Fault
101 rupture impacts for a future Alpine Fault earthquake scenario must therefore be considered as a
102 minimum assessment, with further impacts from currently unknown faults possible.

103

104 **2.2 Landslide impacts**

105 While assessing road impacts from surface fault rupture requires a simple analysis of the locations
106 where roads and faults intersect, identifying potential locations for landslide impacts is more
107 difficult. During the Kaikōura earthquake, landslide road impacts occurred as a result of slippage
108 as well as falling debris (Dellow et al., 2017; Davies et al., 2017). Identifying road sections exposed
109 to landslide impacts therefore requires identifying both where landslide source areas may occur, as
110 well as their corresponding runout paths, which is a difficult and time-consuming task. One way to
111 simplify this is to assess the values of landslide predictor variables in proximity to roads and
112 compare sections that were blocked because of earthquake-induced landslides in a previous
113 earthquake with those that were unaffected. Such an approach can allow mean threshold values of
114 various predictor variables above which all, or the majority, of blockages may occur.

115 The most important predictor variables for landslide occurrence have previously been
116 shown to be some measure of ground shaking (such as Peak Ground Acceleration, PGA), local
117 hillslope gradient and local geology (Parker et al., 2015). This study assesses the average slope
118 angle and ground shaking surrounding roads affected by the 2016 Kaikōura earthquake in order to
119 identify the threshold values above which landslide road impacts occurred. Geology is not
120 considered as most slope failures occurred in greywacke which is the dominant rock type in the
121 area (Massey et al. 2018). This assumes that slopes comprised of schist along the West Coast,
122 where the Alpine Fault is located, will perform similarly to the greywacke slopes north and south of
123 Kaikōura.

124 Ground shaking can be measured using a variety of different variables, including Peak
125 Ground Acceleration (PGA), Peak Ground Velocity (PGV) and Modified Mercalli Intensity (MMI). All
126 three measures of ground shaking are compared for the Kaikōura earthquake (Fig. 1) using data
127 from Bradley et al. (2017a) at 1 km grid resolution. It should be noted however, that the shaking
128 values for the Kaikōura earthquake from Bradley et al. (2017a) differ from those derived by the
129 USGS and ShakeMap NZ models. Nevertheless, scenario outputs for an Alpine Fault earthquake
130 from the USGS and ShakeMap NZ are not available, while outputs using the same model as
131 Bradley et al. (2017a) are available (Bradley et al., 2017b, c); this study therefore uses the Bradley
132 et al. (2017a) outputs to maintain consistency. Slope angle is calculated from the Land Information
133 New Zealand DEM using a grid size of 25 m. It should be noted however, that such a resolution is
134 likely to be coarse to identify small artificial slopes such as road cuts. While these slopes present a
135 notable and local hazard, Mason et al. (2017) highlight that in the Kaikōura earthquake road cut
136 failures were limited to minor rockfall which predominantly resulted in minor impingement of the
137 road course or the blockage of a single lane. This may not, however, be the case for an Alpine
138 Fault earthquake.

139 Affected roads are split into 500 m segments and buffers of 100 m, 250 m, and 500 m are
140 created around each segment. A length of 500 m was chosen to provide a reasonable resolution
141 whilst allowing consistent analysis when applied to the much larger study area for the Alpine Fault
142 earthquake scenario. Buffer widths are selected primarily to account for short-, medium-, and long-
143 landslide runout lengths, with few landslides having runouts > 500 m (Massey et al., 2017). Buffer
144 widths < 100 m are assumed to be meaningful due to the pixel resolution of 25 m. Mean
145 values of ground shaking and slope angle are calculated within each buffer zone and values
146 relating to blocked and unblocked road sections are compared.

147

148 **2.3 An Alpine Fault earthquake scenario**

149 In order to identify potential locations of road impacts from a future Alpine Fault earthquake, first a
150 possible scenario earthquake must be derived. For this study, the scenario used in Project AF8
151 (www.projectaf8.co.nz) has been selected. Project AF8 aims to inform emergency response
152 planning using scenario-based analysis. The scenario developed involves an M_w 7.9 earthquake

153 with ~350 km rupture between Charles Sound and Hokitika (Fig. 1). Ground shaking variables for
154 this scenario have been taken from Bradley et al. (2017b,c) at 1 km grid resolution. The effect of
155 rupture directivity has been considered as part of Project AF8, with three different rupture
156 directions considered: south-to-north, bi-lateral, and north-to-south. In this study, only the south-to-
157 north rupture direction has been considered (Fig. 1) as, at the time of writing, it is the only scenario
158 for which shaking data is openly available. Slope data is calculated using the same dataset and
159 resolution as the Kaikōura dataset for consistency.

160

161 **3 RESULTS**

162 **3.1 Observed blockages from the Kaikōura earthquake**

163 Surface fault rupture crossed SH1 and SH70 at eight locations (Fig. 1). Five of these are located
164 on SH1 as a result of surface rupture on the Kekerengu, Papatea, and Hundalee faults, and three
165 on SH70 from the The Humps, North and South Leader, and Conway-Charwell faults (Stirling et
166 al., 2017). Placing a 50 m buffer around the fault ruptures yields 10 locations, with the two extra
167 locations occurring west of Oaro on SH70 where fault rupture ran parallel and close to the road
168 (Fig. 1). This suggests that a 50 m buffer for the Alpine Fault scenario is appropriate although
169 conservative.

170 Results for the analysis of landslide blockages show there were 20 blocked locations (Fig.
171 2). Notably, regardless of buffer width, all road segments affected by landslides had surrounding
172 slope angles that averaged $> 17^\circ$ and shaking that averaged > 0.43 g (PGA), > 41 cm/s (PGV), or
173 $MM > 7.9$ (MMI) (Fig. 2). By comparison, road segments with mean slope angle and ground
174 shaking values that exceed these thresholds in the scenario Alpine Fault earthquake can therefore
175 be considered at risk of landslide blockage. However, a large number of unblocked road segments
176 also had average slope angles and ground shaking in excess of these thresholds (Fig. 2).

177 To optimise the predictive power of the model, higher thresholds are assigned that
178 simultaneously maximise the number of blocked sections and minimise the number of unblocked
179 sections above both thresholds. The upper threshold slope angle varies with buffer width, with 22°
180 for 100 m buffers, 28° for 250 m buffers, and 25° for 500 m buffers. For the ground shaking
181 variables, buffer width has no effect on upper threshold values, with 0.56 g for PGA, 76 cm/s for
182 PGV, and 8.8 for MMI respectively. If such thresholds were applied to other roads and earthquake
183 scenarios (e.g., an Alpine Fault scenario), it would be possible, with uncertainty, to forecast
184 locations where landslide blockages could be expected.

185 Before doing so, it is important to consider the predictive ability of each threshold
186 combination, particularly in terms of the number of blockages (true positives) as well as the
187 number of unblocked sections (false positives). For the Kaikōura earthquake, a total of 20 road
188 sections were blocked, leaving 634 sections unblocked. A perfect prediction should therefore have
189 all 20 blocked sections above the threshold combination and all 634 unblocked sections below.
190 Data for the thresholds in Figure 2 are summarised in Table 1. The lower threshold combinations

191 for all buffer widths are deliberately set to successfully account for all 20 landslide blocked sections
192 however, these thresholds also result in a large number of false positives, meaning the total
193 number of blocked road sections are in the minority. For instance, using a 250 m buffer and PGA
194 as the shaking predictor, a total of 56 road segments are above the lower thresholds, meaning just
195 36% were actually blocked (Table 1). Using the higher threshold combinations greatly reduces the
196 number of false positives so that the majority of sections above the thresholds are true positives.
197 However, this has the negative effect of reducing the total number of true positives. For instance,
198 using the same example as before, 23 road segments are above the higher thresholds, of which
199 65% were actually blocked; however, 5 blocked segments are below the threshold combination.

200

201 **3.2 Scenario Alpine Fault earthquake**

202 For the scenario Alpine Fault earthquake (Fig. 1), seven sections of State Highway are located
203 within 50 m of a known surface trace of the Alpine Fault (Fig. 3) and thus at risk of blockage in this
204 scenario. The majority of these occur between the townships of Franz Josef and Haast, with a
205 further location between Franz Josef and Hokitika. Surface fault ruptures from previous Alpine
206 Fault earthquakes are thought to have averaged ~8 m horizontally and 1-2 m vertically (Berryman
207 et al., 2012). Such displacements are similar to or larger than those experienced in the Kaikōura
208 earthquake (Stirling et al., 2017) and suggest that these sections of road will be completely
209 impassable to all vehicles.

210 The number and location of road segments exceeding the corresponding upper and lower
211 landslide blockage thresholds from the Kaikōura earthquake (Fig. 2; Table 1) varies between 17
212 and 120 depending on the ground shaking variable and buffer width (Fig. 3). Using PGA
213 consistently yields fewer segments at risk (between 17 and 24) of landslide blockages than PGV
214 (between 54 and 91) or MMI (between 69 and 120). This appears to result from the lack of high
215 PGA values in the Arthur's Pass region compared to high PGV and MMI values (Figs. 1 & 3).
216 Without independent testing of the performance of each shaking variable it is impossible to say
217 which performs best, however, the relative agreement between the PGV and MMI variables
218 suggests the results associated with these measures may be more accurate.

219 In total, for the same shaking variable, the number of segments at risk of blockage generally
220 decreases with decreasing buffer width. This likely relates the fact the majority of road segments
221 for the Alpine Fault scenario are inland and therefore increases in buffer width produce larger
222 changes in average slope angle than on the predominantly coastal roads affected by the Kaikōura
223 event. Nevertheless, despite the variability, several sections of road are consistently at risk of
224 landslide blockage, irrespective of the different buffer widths used. These are:

- 225 • SH6 immediately south of Franz Josef;
- 226 • SH6 ~20 km north-east of Haast;
- 227 • SH6 ~10 km east of Haast;
- 228 • SH94 immediately south of Milford Sound; and

229 • SH73 immediately north of Arthurs Pass.
230 If these sections were blocked, access to the West Coast Region would only be possible via SH7,
231 with access only possible to ~50 km south of Hokitika. Consequently, according to the most recent
232 NZ census (Statistics New Zealand, 2017), > 10,000 local people would be cut-off by road.
233 Depending on the time of year, several thousand domestic and international tourists could also be
234 affected. This is a substantially larger number of people than affected by the Kaikōura earthquake,
235 with the population also being more widely distributed. Further, unlike during the Kaikōura
236 earthquake when alternative access to Blenheim remained possible via SH7, no alternative road
237 routes to Milford Sound, Franz Josef, Haast, or Arthur's Pass exist. Re-establishing connections
238 with these townships is likely to prove a substantial challenge in both the short- and long-term
239 following an Alpine Fault earthquake.

240

241 **4 DISCUSSION**

242 **4.1 Gaining emergency access**

243 Following the Kaikōura earthquake, CDEM immediately prioritised gaining access to isolated
244 communities to provide essential supplies and evacuate stranded tourists in order to reduce the
245 load on what limited local supplies were available (Davies et al., 2017). Due to road blockages, this
246 was possible via only air and sea; however, both options proved unreliable. Poor weather
247 conditions restricted flying and resulted in several days when flying was not possible, while the
248 small size of, and damage to the Kaikōura port restricted the number and size of ships that could
249 dock (Davies et al., 2017). In total 998 tourists were evacuated from Kaikōura either by air or by
250 sea.

251 Similar issues are also expected to occur following an Alpine Fault earthquake. Gaining
252 access to the West Coast Region and Milford Sound is likely to be CDEM's main priority, and with
253 the expected damage to roads (Fig. 3), air and sea routes are likely to provide the only options.
254 However, weather conditions west of the Southern Alps can be difficult and changeable, with
255 monthly average rainfall in Hokitika averaging 250 mm while in Milford Sound this can exceed 500
256 mm, and with rainfall occurring > 200 days per year. Furthermore, few locations in West Coast
257 Region have access to airstrips, meaning they are likely to be reliant on helicopters which have
258 smaller weight carrying capacities than fixed wing aircraft. As in Kaikōura, ports in West Coast
259 Region and Milford Sound are small and likely to have sustained damage during the earthquake,
260 limiting the size and number of ships that can dock. However, no viable berthing spots for ships
261 exist between Hokitika and Milford Sound, meaning isolated communities in this region are likely to
262 be entirely reliant on air access.

263 A further complication exists in the number and location of tourists affected by an Alpine
264 Fault earthquake. While ~1000 tourists were evacuated from Kaikōura following the 2016
265 earthquake, an Alpine Fault earthquake could affect far larger numbers of tourists. Over 1.3 million
266 travellers visit the West Coast Region each year, with enough capacity for up to 4000 visitors per

267 night in the popular Franz Josef area (Tourism West Coast, 2015). Milford Sound is one of New
268 Zealand's most popular tourist sites, attracting > 650,000 visitors per year, equating to ~1700 per
269 day (Venture Southland, 2017). While at night visitors cluster to major townships, during the day
270 most will be spread out across the region, with many visiting remote areas on foot. Consequently,
271 it is possible that following an Alpine Fault earthquake, nearly five times as many tourists will
272 require evacuation compared to the Kaikōura earthquake, with these people distributed across a
273 region > 10,000 km².

274

275 **4.2 Restoration and recovery**

276 New Zealand Transport Agency (NZTA) began clearing road blockages 2 days after the Kaikōura
277 earthquake, focussing initially on SH70 and SH1 south of Kaikōura (Davies et al., 2017). The focus
278 was primarily to return road access to all isolated communities and allow emergency vehicles
279 access to affected regions. However, it took 11 days before non-emergency vehicles could leave
280 Kaikōura via supervised convoy on SH70 (Davies et al., 2017). It took 23 days to restore
281 supervised access to all isolated communities, with SH70 becoming the first road fully re-opened
282 after 38 days. SH1 was finally re-opened in December 2017, albeit only to single-file traffic during
283 daylight hours and in dry weather conditions.

284 Restoring road access following an Alpine Fault earthquake is likely to prove as difficult as
285 the northern section of SH1. While access to the West Coast Region is likely to remain possible via
286 SH7 (Fig. 3), restoring access along SH6 and SH73 is expected to prove difficult due to the steep
287 terrain, likelihood of poor weather, and continuing aftershocks. Further considerations for
288 restoration times include whether or not the road is confined, the volume of debris to remove and
289 the ease of access. Reopening the alpine passes will prove most difficult, as the confined nature
290 means rerouting the road is not an option and thus landslide debris will need to be removed.
291 Further, the narrow nature of the passes means that debris clearance will likely be restricted to the
292 outer-most blocking landslides, with limited options for simultaneous clearance of multiple landslide
293 blockages. Previous estimates by NZTA have therefore suggested it would require > 6 months
294 before restoration works could even begin on SH6 south of Franz Josef and east of Haast, and on
295 SH73 (Robinson et al., 2015). Given the difficulties being experienced clearing SH1 north of
296 Kaikōura these estimates appear to be realistic, if not under-estimates. This means no road access
297 is expected on SH6 between Franz Josef and Haast, and along SH73 for > 6 months after an
298 Alpine Fault earthquake. In comparison, SH94 is expected to be cleared within 14 days as the
299 route is regularly blocked by avalanches and rockfalls and consequently NZTA are experienced at
300 clearing this route and have sufficient equipment already in place (Robinson et al., 2015). It should
301 be noted here however, that road bridge performance has not been accounted for here, and a
302 collapse of a major road bridge is likely to present as large a challenge for restoration as landslide
303 or surface fault rupture.

304

305 **4.3 Implications for emergency response**

306 The Kaikōura earthquake provides a useful analogue for a future Alpine Fault earthquake in terms
307 of road impacts and loss of access. It therefore provides an opportunity to evaluate the emergency
308 response undertaken and plan the necessary future response. Firstly, it is clear that planning for
309 the evacuation of large numbers of spatially distributed tourists is essential. In the 2016
310 earthquake, tourists were evacuated from Kaikōura township by a combination of air and sea, with
311 363 evacuated by helicopter and 635 by sea (Davies et al., 2017). This evacuation was partly
312 aided by tourists being concentrated in a single township, however in an Alpine Fault earthquake
313 larger numbers of tourists are expected to be distributed across a much larger area, especially if it
314 occurs during the daytime. This is in conjunction with an expectation that weather conditions in
315 West Coast Region are likely to hinder air evacuations and the lack of sufficient port facilities will
316 hinder evacuations by sea. It is therefore essential that contingency planning for the evacuation of
317 tourists following an Alpine Fault earthquake is undertaken.

318 A further key issue is in the provision of emergency supplies to isolated local populations.
319 While the current MCDEM advice is to be self-sufficient for 3 days following a disaster, it is clear
320 that many West Coast communities will be isolated for far longer following an Alpine Fault
321 earthquake. As in the Kaikōura earthquake, ensuring emergency supplies can be delivered to
322 these regions is essential. While initially this may be able to be combined with evacuation of
323 tourists, with some road routes expected to be impassable for > 6 months, continuous resupply by
324 sea and air is unlikely to be sustainable. Considering alternative arrangements is therefore
325 essential. One possibility is the temporary evacuation of isolated local populations until road
326 access can be restored. However, this is likely to prove controversial and poses questions as to
327 how to respond to anyone refusing to leave as well as the management of safe return. Planning
328 how to maintain supplies to isolated locals for several months following an Alpine Fault earthquake
329 is therefore urgently required.

330 A final implication to consider is the effect of such road impacts on the local economy. The
331 West Coast Region has three major industries: mining, tourism, and dairy. Mining is predominantly
332 dependant on the rail network, which has not been investigated in this study. However, the main
333 rail route that transports mining products to Christchurch for national and international distribution
334 follows SH73 for much of its route and therefore is also expected to be severely impacted. The
335 loss of reliable road access to much of the region will undoubtedly affect the dairy and tourism
336 industries, with farms unable to distribute milk products and tourists unable to reach popular
337 destinations such as Franz Josef. While some work has been done to investigate the potential
338 impact of an Alpine Fault earthquake on tourism (Orchiston, 2012), to date little work has looked at
339 the potential impacts to the dairy industry.

340

341 **5 CONCLUSIONS**

342 In terms of its impacts, particularly to roads, the 2016 Kaikōura earthquake provides a potential
343 analogue for a future rupture of the Alpine Fault. The 2016 Kaikōura earthquake displaced major
344 state highways in several locations making the roads completely impassable. Numerous landslides
345 also blocked key access routes, causing many communities to be isolated and requiring the
346 evacuation of tourists by air and sea. An analysis of the predictive variables for landslide
347 occurrence along the SH1 and SH70 road corridors show that the lower and upper thresholds
348 respectively for road blockages were 15° and 28° for local slope, 0.43 g and 0.56 g for PGA, 41
349 cm/s and 76 cm/s for PGV, and 7.9 and 8.8 for MMI. Using these observations, this study identifies
350 up to 120 other locations where landslides may potentially block roads in a future Alpine Fault
351 earthquake. This suggests that blockages can be expected along SH6 between Hokitika and
352 Haast, on SH94 before Milford Sound, and on SH73 around Arthur's Pass. Previous studies have
353 suggested several sections of these roads could take > 6 months to restore. However, it is notable
354 that the number of potential blockage sites varies considerably with different shaking variables,
355 and the length of blockage time is dependent on numerous local factors, which this study has not
356 investigated. Nevertheless, contingency planning for the evacuation of large numbers of spatially
357 distributed tourists and the provision of sufficient emergency supplies to local populations is
358 urgently required. Examining the response to the Kaikōura earthquake may therefore highlight
359 valuable lessons that can be learnt prior to an Alpine Fault earthquake to aid such planning.

360

361 **ACKNOWLEDGEMENTS**

362 I would like to acknowledge Dr Sam McColl and another anonymous reviewer whose helpful
363 feedback greatly improved the quality and scope of this manuscript. This work was undertaken as
364 part of funding provided by the EU Seventh Framework under the COFUND scheme with Durham
365 University.

366

367 **REFERENCES**

- 368 Berryman, K. R., Cochran, U. A., Clark, K. J., Biasi, G. P., Langridge, R. M., & Villamor, P. (2012). Major earthquakes
369 occur regularly on an isolated plate boundary fault. *Science*, 336(6089), 1690-1693.
- 370 Biasi, G. P., Langridge, R. M., Berryman, K. R., Clark, K. J., & Cochran, U. A. (2015). Maximum-Likelihood Recurrence
371 Parameters and Conditional Probability of a Ground-Rupturing Earthquake on the Southern Alpine Fault, South
372 Island, New Zealand. *Bulletin of the Seismological Society of America*, 105(1), 94-106.
- 373 Bradley, B. A., Razafindrakoto, H. N., & Polak, V. (2017) Ground motion observations from the 14 November 2016 Mw
374 7.8 Kaikōura, New Zealand, earthquake and insights from broadband simulations. *Seismological Research Letters*,
375 88, 740-756.
- 376 Bradley, B. A., Bae, S. A., Polak, V., Lee, R. L., Thomson, E. M., & Tarbali, K. (2017b). Ground motion simulations of
377 great earthquakes on the Alpine Fault: effect of hypocentre location and comparison with empirical modelling. *New
378 Zealand Journal of Geology and Geophysics*, 60(3), 188–198.
- 379 Bradley, B., A., Lagrava, D., Savarimuthu, S., & Bae S., E. (2017c). SeisFinder: A web application for the extraction of
380 high-fidelity outputs from computationally-intensive earthquake resilience calculations. QuakeCoRE Annual Meeting,
381 September 2017

382 Cochran, U. A., Clark, K. J., Howarth, J. D., Biasi, G. P., Langridge, R. M., Villamor, P., Berryman, K. R., & Vandergoes,
383 M. J. (2017). A plate boundary earthquake record from a wetland adjacent to the Alpine fault in New Zealand refines
384 hazard estimates. *Earth and Planetary Science Letters*, 464, 175-188.

385 Cubrinovski, M., Bray, J. D., de la Torre, C., Olsen, M. J., Bradley, B.A., Chiaro, G., Stocks, E., & Wotherspoon, L.,
386 (2017). Liquefaction effects and associated damages observed at the Wellington Centreport from the 2016 Kaikōura
387 earthquake. *Bulletin of the New Zealand Society for Earthquake Engineering*, 50(2), 152-173.

388 Davies, A. J., Sadashiva, V., Aghababaei, M., Barnhill, D., Costello, S. B., Fanslow, B., et al. (2017). Transport
389 infrastructure performance and management in the South Island of New Zealand, during the first 100 days following
390 the 2016 Mw 7.8 Kaikōura earthquake. *Bulletin of the New Zealand Society for Earthquake Engineering*, 50(2), 271-
391 299.

392 De Pascale, G. P., & Langridge, R. M. (2012). New on-fault evidence for a great earthquake in AD 1717, central Alpine
393 fault, New Zealand. *Geology*, 40(9), 791-794.

394 Dellow, S., Massey, C., Cox, S., Archibald, G., Begg, J., Bruce, Z., et al. (2017). Landslides caused by the 14 November
395 2016 Mw7. 8 Kaikōura earthquake and the immediate response. *Bulletin of the New Zealand Society for Earthquake*
396 *Engineering*, 50(2), 106-116.

397 Hamling, I. J., Hreinsdóttir, S., Clark, K., Elliott, J., Liang, C., Fielding, E., et al. (2017). Complex multifault rupture during
398 the 2016 Mw 7.8 Kaikōura earthquake, New Zealand. *Science*, 356(6334).

399 Howarth, J. D., Fitzsimons, S. J., Norris, R. J., & Jacobsen, G. E. (2012). Lake sediments record cycles of sediment flux
400 driven by large earthquakes on the Alpine fault, New Zealand. *Geology*, 40(12), 1091-1094.

401 Howarth, J. D., Fitzsimons, S. J., Norris, R. J., Langridge, R., Vandergoes, M. J. (2016). A 2000 yr rupture history for the
402 Alpine fault derived from Lake Ellery, South Island, New Zealand. *Geological Society of America Bulletin*, 128, 627-
403 643, doi:10.1130/B31300.1.

404 Kaiser, A., Balfour, N., Fry, B., Holden, C., Litchfield, N., Gerstenberger, M., et al. (2017). The 2016 Kaikōura, New
405 Zealand, Earthquake: Preliminary Seismological Report. *Seismological Research Letters*, 88(3), 727-739.

406 Liu, Y., Nair, N-K., Renton, A., & Wilson, S. (2017). Impact of the Kaikōura earthquake on the electrical power system
407 infrastructure. *Bulletin of the New Zealand Society for Earthquake Engineering*, 50(2), 300-305.

408 Mason, D., Brabharan, P. & Saul, G. (2017) Performance of road networks in the 2016 Kaikōura earthquake:
409 Observations on ground damage and outage effects. Proc. 20th NZGS Geotechnical Symposium. Eds. GJ
410 Alexander & CY Chin, Napier.

411 Massey, C., Townsend, D., Rathje, E., Allstadt, K. E., Lukovic, B., Kaneko, Y., Bradley, B., Wartman, J., Jibson, R. W.,
412 Petley, D. N., Horspool, N., Hamling, I., Carey, J., Cox, S., Davidson, J., Dellow, S., Godt, J. W., Holden, C., Jones,
413 K., Kaiser, A., Little, M., Lyndsell, B., McColl, S., Morgenstern, R., Rengers, F. K., Rhoades, D., Rosser, B., Strong,
414 D., Singeisen, C., Villeneuve, M. (2017). Landslides Triggered by the 14 November 2016 MwMw 7.8 Kaikōura
415 Earthquake, New Zealand. *Bulletin of the Seismological Society of America* doi: [https://doi-](https://doi-org.ezphost.dur.ac.uk/10.1785/0120170305)
416 [org.ezphost.dur.ac.uk/10.1785/0120170305](https://doi-org.ezphost.dur.ac.uk/10.1785/0120170305)

417 Orchiston, C. (2012). Seismic risk scenario planning and sustainable tourism management: Christchurch and the Alpine
418 Fault zone, South Island, New Zealand. *Journal of Sustainable Tourism*, 20(1), 59-79.

419 Orense, R. P., Mirjafari, Y., Asadi, S., Naghibi, M., Chen, X., Altaf, O., & Asadi, B. (2017). Ground performance in
420 Wellington waterfront area following the 2016 Kaikōura earthquake. *Bulletin of the New Zealand Society for*
421 *Earthquake Engineering*, 50(2), 142-151.

422 Palermo, A., Liu, R., Rais, A., McHaffie, B., Andisheh, K., Pampanin, S., Gentile, R., Nuzzo, I., Granerio, M., Loporcaro,
423 G., McGann, C., & Wotherspoon, L. (2017). Performance of road bridges during the 14 November 2016 Kaikōura
424 earthquake. *Bulletin of the New Zealand Society for Earthquake Engineering*, 50(2), 253-270.

425 Parker, R. N., Hancox, G. T., Petley, D. N., Massey, C. I., Densmore, A. L., & Rosser, N. J. (2015). Spatial distributions
426 of earthquake-induced landslides and hillslope preconditioning in the northwest South Island, New Zealand. *Earth*
427 *Surface Dynamics*, 3(4), 501.

428 Robinson, T. R., & Davies, T. R. H. (2013). potential geomorphic consequences of a future great (Mw= 8.0+) Alpine Fault
429 earthquake, South Island, New Zealand. *Natural Hazards and Earth System Sciences*, 13(9), 2279.

430 Robinson, T. R., Wilson, T. M., Buxton, R., Cousins, W. J., & Christophersen, A. M. (2015) An Alpine Fault earthquake
431 scenario to aid in the development of the Economics of Resilient Infrastructure's MERIT model. ERI Research
432 Report 2016/04.

433 Robinson, T. R., Davies, T. R. H., Wilson, T. M., & Orchiston, C. (2016). Coseismic landsliding estimates for an Alpine
434 Fault earthquake and the consequences for erosion of the Southern Alps, New Zealand. *Geomorphology*, 263, 71-
435 86.

436 Statistics New Zealand (2017). Subnational population estimates: at 30 June 2017 (provisional). Retrieved from
437 nzdotstat.stats.govt.nz/wbos/Index.aspx?DataSetCode=TABLECODE7541. Last Accessed 28 March 2018.

438 Stirling, M., McVerry, G., Gerstenberger, M., Litchfield, N., Van Dissen, R., Berryman, K., Barnes, P., Wallace, L.,
439 Villamor, P., Langridge, R., Lamarche, G., Nodder, S., Reyners, M., Bradley, B., Rhoades, D., Smith, W., Nicol, A.,
440 Pettinga, J., Clark, K., Jacobs, K. (2012). National Seismic Hazard Model for New Zealand: 2010 Update. *Bulletin of*
441 *the Seismological Society of America*, 102 (4): 1514–1542. doi: <https://doi.org/10.1785/0120110170>

442 Stirling, M. W., Litchfield, N. J., Villamor, P., Van Dissen, R. J., Nicol, A., Pettinga, J., et al. (2017). The Mw7. 8 2016
443 Kaikōura earthquake: Surface fault rupture and seismic hazard context. *Bulletin of the New Zealand Society for*
444 *Earthquake Engineering*, 50(2), 73-84.

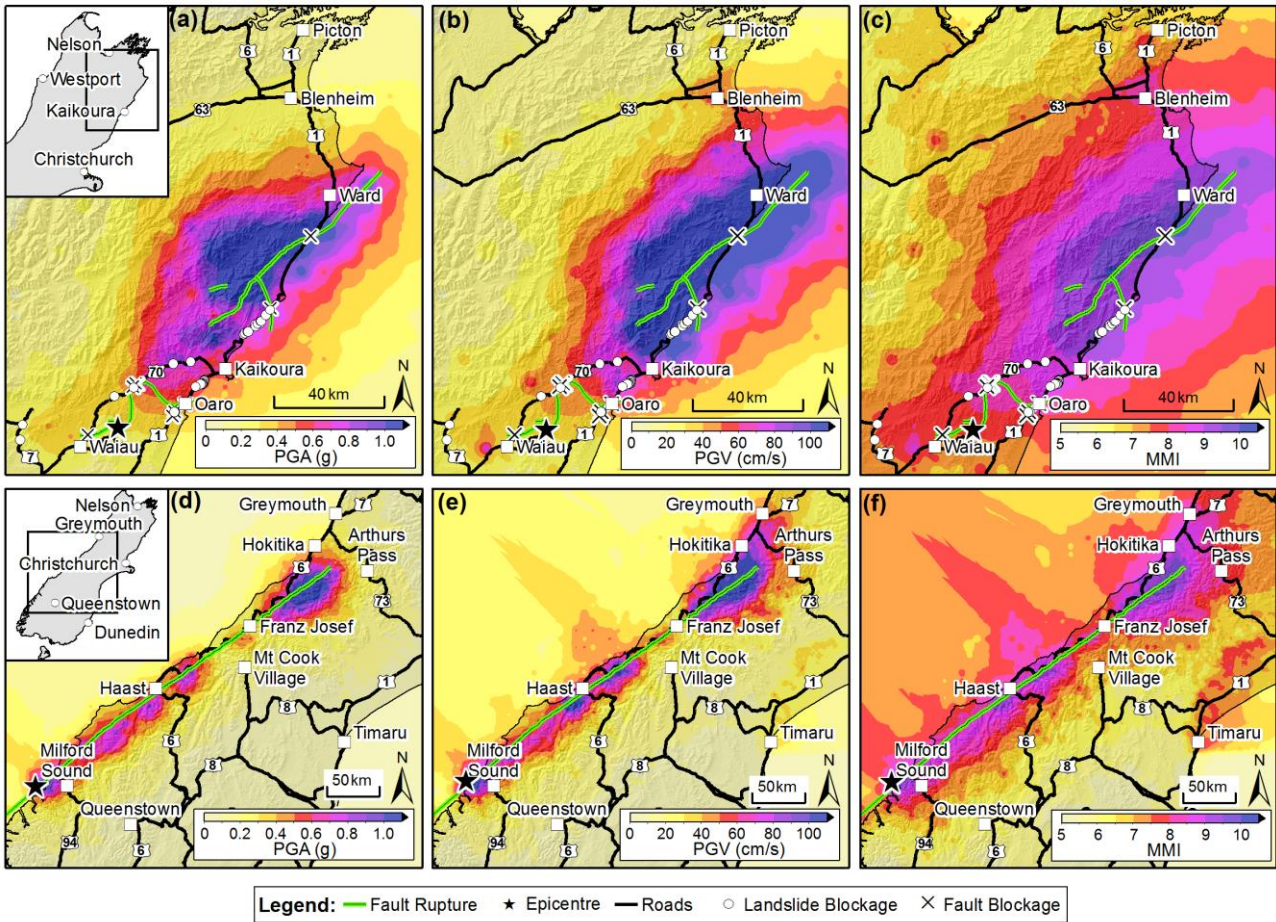
445 Tourism West Coast (2015) Minutes of the Annual General Meeting of Tourism West Coast Inc. 5th July 2015.

446 Venture Southland (2017) Southland tourism key indicators. MBIE Report.

447 Wells, A., Yetton, M. D., Duncan, R. P., & Stewart, G. H. (1999). Prehistoric dates of the most recent Alpine fault
448 earthquakes, New Zealand. *Geology*, 27(11), 995-998.

449 Yetton, M. D. (1998). Progress in understanding the paleoseismicity of the central and northern Alpine Fault, Westland,
450 New Zealand. *New Zealand Journal of Geology and Geophysics*, 41(4), 475-483.

451



453

454

455

456

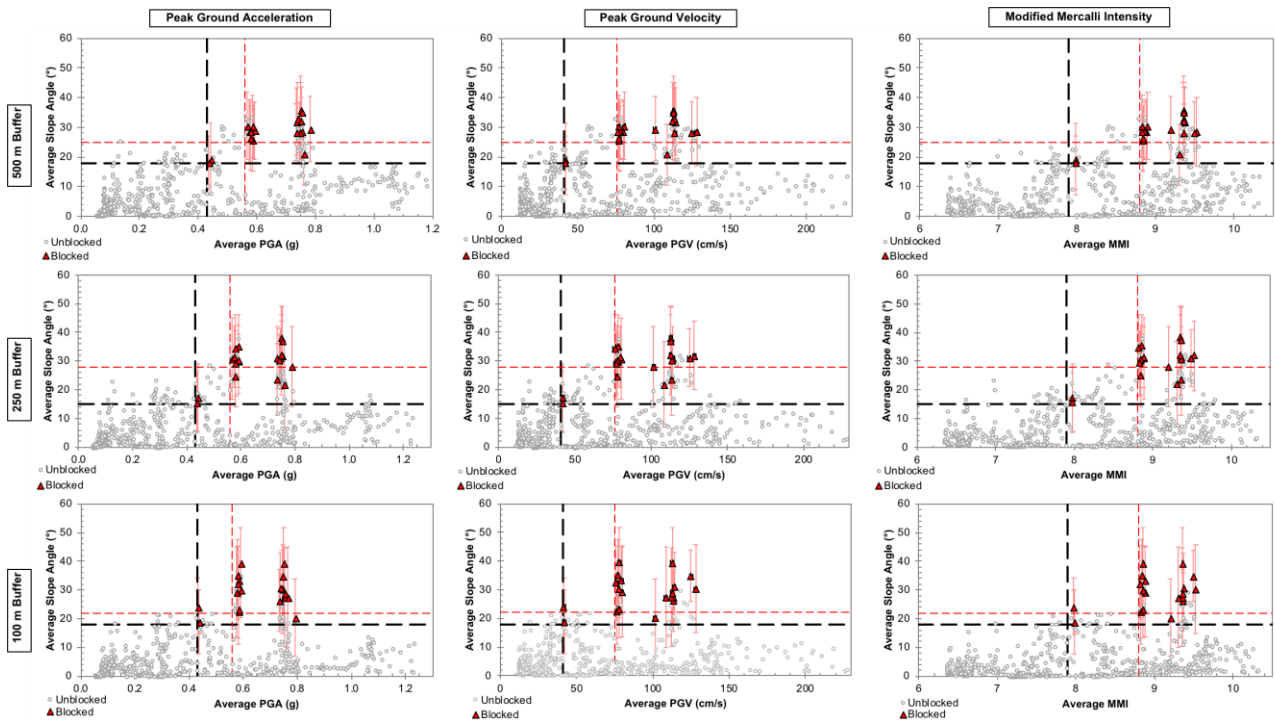
457

458

459

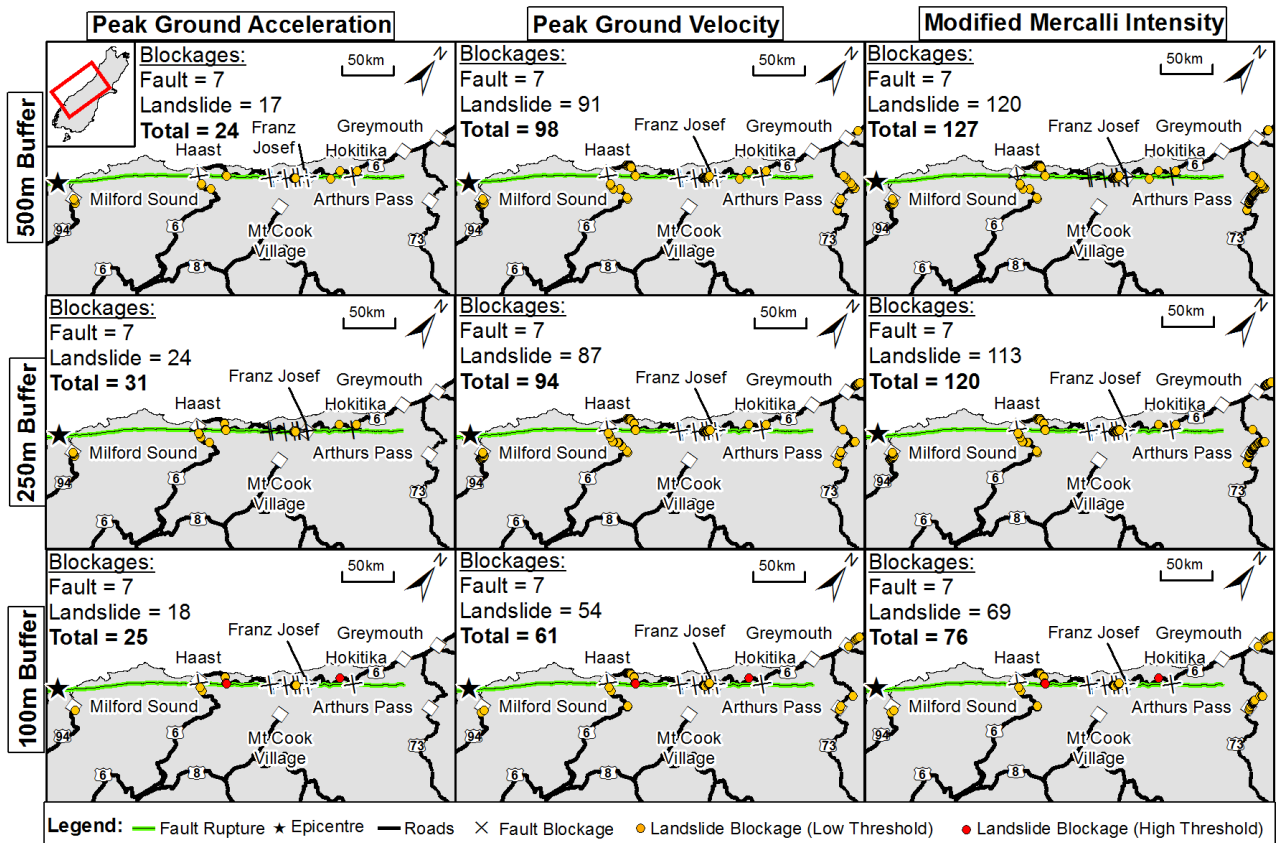
460

Figure 1 – Road Impacts and various measures of ground shaking from the 2016 M_w 7.8 Kaikōura earthquake (Bradley et al., 2017a) compared to a proposed M_w 7.9 Alpine Fault earthquake scenario rupturing from south to north (Bradley et al., 2017b,c) developed for project AF8 (www.projectaf8.co.nz). (a-c) PGA (a), PGV (b) and MMI (c) from the Kaikōura earthquake; (d-e) PGA (d), PGV (e) and MMI (f) for the scenario Alpine Fault earthquake. Inset (a) – location of (a-c) within the upper South Island. Inset (d) – location of (d-f) within the South Island.



461
 462
 463
 464
 465
 466
 467
 468
 469

Figure 2 – Average slope angle compared to average PGA, PGV, and MMI values within 500 m, 250 m, and 100 m buffers for each 500 m section of road network between Christchurch and Picton. Sections blocked by landslides are shown in red with the total range of variable shown by error bars. Sections unaffected by landslides are shown in grey. Black dashed lines represent lower threshold values above which 100% of landslide blockages occur. Red dashed lines represent upper threshold values maximising the number of landslide blockages above the thresholds (true positives) whilst minimising the number of unblocked sections above the thresholds (false positives).



470

471

Figure 3 – Locations of road impacts related to surface fault rupture and landslides from an Alpine Fault earthquake for different buffer widths and shaking variables. Threshold data for landslide blockages are calculated from observations of the Kaikōura earthquake from Fig. 2 and Table 1.

472

473

474

475

476 **TABLES**

477 **Table 1** – Upper and lower thresholds and corresponding prediction scores derived from Fig. 2 for different buffer widths
 478 and ground shaking variables for landslide road blockages during the 2016 Kaikōura earthquake. TP – true positives,
 479 number of blocked sections above the corresponding thresholds; FP – false positives, number of unblocked sections
 480 above the corresponding thresholds.

	Buffer Width (m)	Shaking Threshold	Slope Threshold	TP (/20)	FP (/634)
PGA (g)	100	0.43	17°	20	20
	250	0.43	17°	20	36
	500	0.43	17°	20	38
	100	0.56	22°	17	10
	250	0.56	28°	15	8
	500	0.56	25°	17	15
PGV (cm/s)	100	41	17°	20	23
	250	41	17°	20	42
	500	41	17°	20	45
	100	76	22°	17	10
	250	76	28°	14	7
	500	76	25°	17	14
MMI	100	7.9	17°	20	24
	250	7.9	17°	20	44
	500	7.9	17°	20	46
	100	8.8	22°	17	10
	250	8.8	28°	15	7
	500	8.8	25°	17	14

481

482